LETTERS

OPTICAL IMAGING OF EDGE TURBULENCE IN THE CALTECH TOKAMAK

S.J. ZWEBEN, J. McCHESNEY, R.W. GOULD
(Department of Applied Physics, California Institute of Technology, Pasadena, California, United States of America)

ABSTRACT. A linear photodiode array is used to image visible-light emission from the edge plasma of the Caltech Tokamak. The patterns of light fluctuation show small-scale broadband structure similar to that previously measured for plasma edge density turbulence. A high correlation is found between these light fluctuations and the fluctuations measured by a nearby Langmuir probe.

1. INTRODUCTION

Recently, high-speed movie films have been made of the visible-light emission from the ASDEX, DITE, and DIVA tokamaks [1, 2]. These films have shown several remarkable features including violent plasma instabilities during start-up and discharge disruption, and bright localized 'UFOs' which are associated with the evaporation of small metallic particles. However, for macroscopically stable discharges the visible light comes mainly from H_α in the plasma edge where the temperature is low and the neutral-hydrogen density is high.

During the periods of macroscopic stability, a surprisingly distinct pattern of 'filamentation' is observed in the visible emission from the plasma edge. In particular, the ASDEX films show these filaments to be highly elongated in the toroidal direction (> 1 m) and very short and irregularly spaced in the poloidal direction (~ 5 cm). Since the filaments fluctuate in position from frame to frame, independent of the filming speed (up to 7000 frames per second) and their poloidal scale-lengths are much smaller than the minor radius, it is natural to associate them with the plasma edge turbulence previously measured in tokamaks with CO_2 and microwave scattering [3, 4] and with Langmuir probes [5, 6].

In this paper, we make this connection explicit and show that these visible-light fluctuations are well correlated with edge density fluctuations measured nearby with a Langmuir probe. The photodiode array used to monitor the visible fluctuations also allows a more quantitative analysis of the turbulence patterns than does the film, and the non-perturbative nature of the measurement makes it possible to use this technique as a simple diagnostic of edge plasma turbulence in large tokamaks.

2. EXPERIMENTAL ARRANGEMENT

The visible-light emission was viewed radially through a port at the outer equatorial plane of the Caltech Research Tokamak ($B = 3.5$ kG, $I = 20$ kA, $R = 45$ cm, $a - 16$ cm, $\bar{n} = 10^{12} - 10^{13}$ cm^{-3}). As shown in Fig. 1, a linear array of 16 fast photodiodes (Fairchild FPT102) was aligned vertically to view a poloidally extended slice of the plasma through a single f/1.6 lens system. Alignment and focusing were done by using an incandescent filament located at the end of a shaft near the top of the array. The same shaft also held a 1-cm-long, 0.1-cm-diameter Langmuir probe, which was used for the local measurement of edge density fluctuations.

The 'object' focused onto the photodiode array was located at the outer edge of the chamber ($R = R_0 + a$) so as to obtain good spatial resolution in the plasma edge region. At the outer edge the array viewed a total area 8 cm high ($\pm 15°$ about the equatorial plane in the poloidal direction) by 0.3 cm wide (in the toroidal direction), such that fields of view of adjacent diodes in this plane were centred 0.5 cm apart poloidally. A single diode viewed an area of about 0.3 cm diameter in the object plane, so that its view in the edge region did not overlap with that of an adjacent diode.

Although the photodiode array was aligned so as not to see the sides of the flange between itself and the plasma, it did see the far wall of the chamber. However, since the metal surface of the chamber was quite rough, the reflected light from it would be expected to add only a globally averaged (non-fluctuating) component to the directly viewed plasma light.

Also, each photodiode actually views a cone centred on the focal point and extending through the plasma (see Fig. 1), so that its signal is composed of an average of the emission in its direction over this cone. However, since the area it viewed expanded rapidly away from the focal point (e.g. it has a diameter of about 9 cm at the inner edge at $R = R_0 - a$), the contributions due to small-scale structure away from the focus will be spatially averaged, and so should contribute mainly a constant level to the diode's signal.

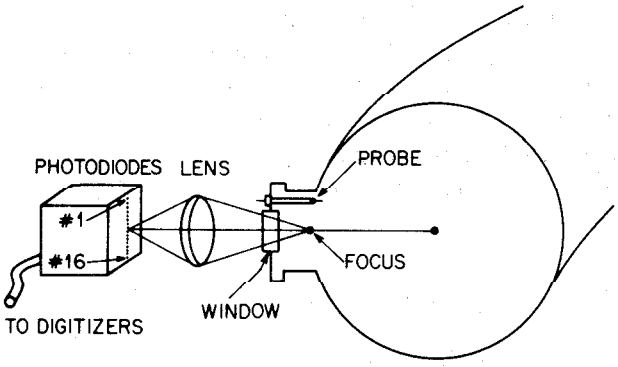

FIG.1. Experimental arrangement showing point at outer equatorial plane imaged onto centre of the photodiode array. Langmuir probe can be placed at focus of photodiode #15.

For a precise unfolding of the array signals, one would need to know the radial profile of the visible emissivity of the plasma. This is not measured in the present experiment, because of lack of full poloidal access; however, it was indicated by insertion of a red ($\lambda \gtrsim 6000$ Å) filter that over 50% of the received light comes from H_α, which is expected to be excited only in the cool-plasma edge region. In ASDEX, it was estimated that the visible light came from H_α within a ring of width 3 cm at the edge [1].

Thus we can make the approximate interpretation for this experiment that any small-scale fluctuating components of the array signals are due to fluctuations in the local emissivity in the outer edge region. The non-fluctuating component of these signals can come from either the direct emission from the outer edge, from reflected light from the far wall, or from spatially averaged emission from the rest of the diode's field of view.

The local emissivity is, in general, determined by the plasma density, temperature, and composition according to:

$$L(n_i, n_e, T_e) = \sum_i n_i n_e f_i(T_e) \qquad (1)$$

where n_i is the density of species 'i', n_e the electron density, and $f_i(T_e)$ some complicated function determined by the atomic physics of that species. Equation (1) is strictly true only if the atoms are in equilibrium with the local plasma; if not, the local emissivity also depends on the transport processes affecting that species. For the emission due to neutral hydrogen, however, we can assume that the local neutral density is not fluctuating, so that the emissivity would at least be linearly proportional to the local electron density.

The 16-photodiode signals are recorded on two LeCroy 2264 eight-channel eight-bit digitizers at a sampling rate of 400 kHz for each channel. The photodiodes themselves have a flat frequency response to 1 MHz; however, since there was very little signal above 100 kHz, the LM308 amplifiers of the diode were adjusted to have a frequency response of about 150 kHz to avoid aliasing in the digitizer. The fluctuating component of the digitized signals was typically 10 – 100 times the total system noise level for frequencies below 100 kHz. The cross talk between channels and possible electromagnetic pick-up from the machine were checked to be negligible by blocking individual diodes during a shot.

The tungsten Langmuir probe tip was intentionally made longer than usual to radially average over fluctuations within the outer edge region. The probe was biased typically -125 V with respect to the local chamber ground, i.e. well into the ion saturation current region. The probe current I_s should be linearly proportional to the local density, but might also respond to fluctuations in temperature proportionally to $\sqrt{T_e}$ (see Section 5).

3. ARRAY SIGNALS

In Fig.2, a typical signal from one of the photodiodes (# 9) is shown, together with the plasma current, the line-averaged density, the total UV emission measured along a chord through the minor axis [7], and the ion saturation current I_s measured by the Langmuir probe in the edge plasma near the focus of photodiode # 15. In this case, there was no localized limiter in the plasma and the probe tip was inserted 0.5 cm radially in past the outer wall. When an 8-cm-high outer limiter was inserted 2 cm at 60° downstream, the shapes of these signals changed somewhat, because of the different re-cycling, but the relative fluctuation levels remained about the same.

The large initial peak in the visible signal is due to the ionization of H^0 during the breakdown phase of the discharge, and the steady level during the middle of the discharge is associated mainly with H_α, owing to gas puffing. The gas puffing valve is located 120° toroidally and 90° poloidally from the photodiode's field of view, so is not seen directly. The ratio of the breakdown peak to the steady-state light level is about 10:1, indicating that the bulk of the plasma is

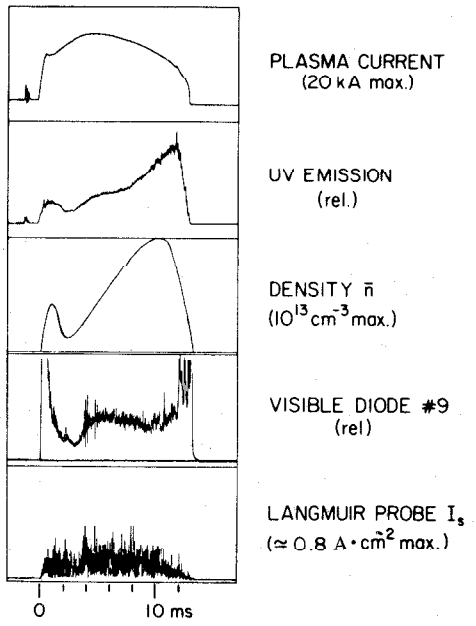

FIG.2. Signals from tokamak during limiterless discharge with gas puffing. Visible photodiode shows 6 – 9% fluctuations, while Langmuir probe 0.5 cm into plasma shows 50% rms fluctuations.

fully ionized during steady state. The increased light signal at the end of the discharge is due to plasma-wall contact initiated by the disruption which occurs at the density limit.

The region of interest for the present experiment is during the middle part of the discharge from $t = 4 - 10$ ms. During this period, the photodiode signal is observed to have a 6 – 9% rms fluctuation level, which is more than ten times larger than the total system noise level. These visible light fluctuations are present during all discharges observed, with or without limiters and for the whole range of density available of this machine.

The fluctuations in ion saturation current are relatively much larger, typically 50% rms. Qualitatively speaking, this is explained by the fact the probe samples only the edge plasma fluctuations, while the photodiodes respond to the edge plus the averaged light emission from the rest of their field of view (see Section 1).

In Fig.3, the signals from 15 photodiodes in the array are shown for an expanded portion of the middle of a discharge like that of Fig.2 ($t \approx 6$ ms). The amplitudes were each normalized to the peak light emission during breakdown to remove variations due to the differing photodiode sensitivities. Only the 6 – 9% rms fluctuating components of the light are displayed in this plot. The space-time patterns shown in this figure are typical of those seen during the macroscopically stable (low-MHD) rising density portion of the discharge at $t = 4 - 10$ ms.

Several general features of these space-time patterns can be seen in the raw data. In the first place, it is evident that the signals fluctuate irregularly in time and contain many frequency components. As described below, the auto-correlation times for individual signals are very short, as is typical of turbulence. Also evident is that many of the small features have a very short spatial correlation length, extending typically 4 – 8 diodes or 2 – 4 cm in the poloidal direction. On the other hand, there are also features which extend relatively undistorted across the whole array, although these are not spaced regularly in time as would be the case for large-scale coherent modes (see Section 5). Altogether, the space-time visible light patterns seen in Fig.3 (and in many similar examples) appear to be dominated by small-scale turbulence similar to that visible in the ASDEX films, at least for these macroscopically stable discharge conditions.

For a more quantitative analysis of these data, we have calculated auto- and cross-correlation functions in the time domain and auto- and cross-power spectra and coherences in the frequency domain. Some typical results are presented in Fig.4.

Figure 4a shows the normalized cross-correlation functions (L_{16}, L_n) between the signal from one diode

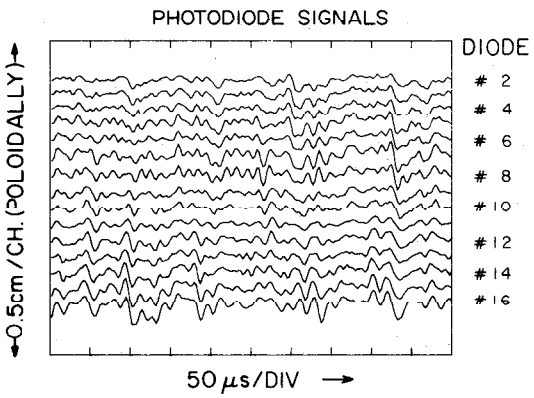

FIG.3. Fluctuation pattern as observed by photodiode array during middle of discharge like that in Fig.2. Most high-frequency features have short poloidal correlation length, while lower-frequency features have longer poloidal correlation length.

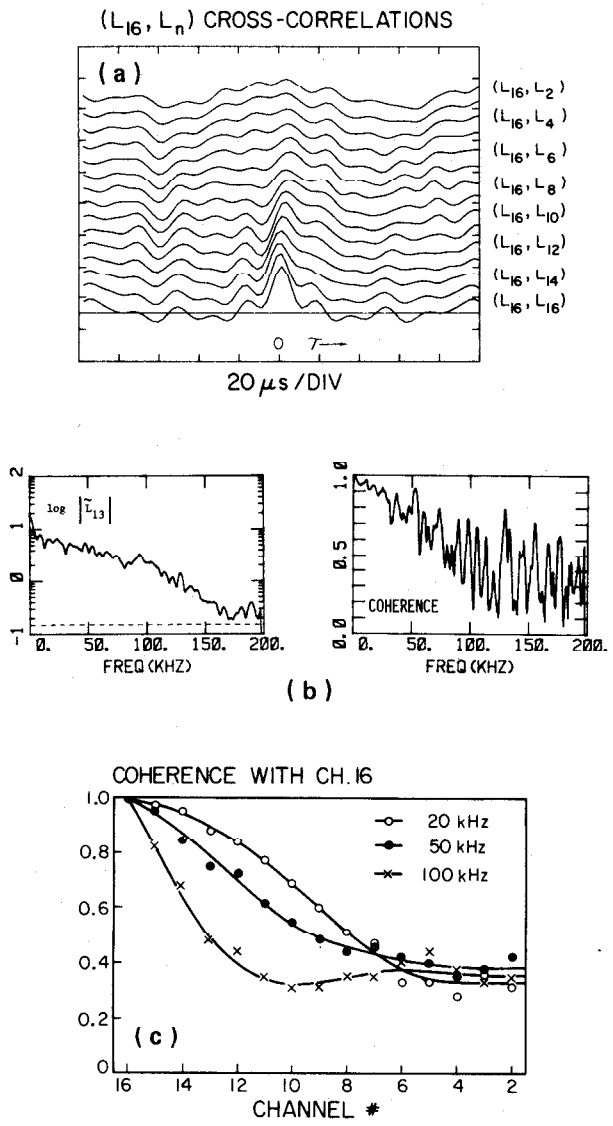

FIG.4(a). Cross-correlation functions between photodiode #16 and other diodes. Correlation deteriorates in space over 4–8 diodes or 2–4 cm poloidally, and over 10μs in time; (b) frequency spectrum of amplitude of fluctuations from typical diode (system noise shown by dashed line) and coherence spectrum between diode #16 and #13; (c) coherence between diode #16 and other diodes for three frequency ranges, showing that higher frequencies have shorter correlation lengths (coherence of ≅ 0.35 can be expected for totally uncorrelated signals with this level of averaging).

(# 16) and the rest of the array, where for a delay time τ [8]:

$$(L_{16}, L_n) = \frac{T}{(T-\tau)} \sum_{0}^{T-\tau} L_{16}(t)\, L_n(t-\tau) \Bigg/ \sqrt{\sum_{0}^{T} L_{16}^2 \cdot \sum_{0}^{T} L_n^2} \qquad (2)$$

The averaging interval for these signals is T = 500 μs for the cases shown. The bottom trace is the auto-correlation function (L_{16}, L_{16}) from which the auto-correlation time of $\tau_A \cong 10\mu s$ can be obtained. The fact that τ_A is comparable to a typical inverse frequency in this bandwidth indicates that this signal has the character of random noise, i.e. that it does not have any strong long-time correlations such as might be associated with coherent modes. The cross-correlation functions show that the band-averaged spatial correlation of these disturbances is about 4 cm in the poloidal direction, which is much smaller than the minor radius scale length (a = 16 cm) and again indicates the similarity of these light patterns to the small-scale turbulence observed in the films and in the probe measurements (6).

Figure 4b shows examples of the frequency spectrum of a diode (L_{13}) and the frequency-resolved coherence spectrum between two nearby diodes (L_{16} and L_{13}). Both spectra are Gaussian-averaged over 6-kHz FWHM for this analysis [6, 8]. The visible fluctuation spectra are broadband up to about 100 kHz and typically have an exponential shape in this range. The coherence between two directly adjacent diodes is always very high (above 90%) for all frequencies below 100 kHz. However, as shown, for example, in Fig.4b for a diode focus separation of 1.5 cm, the coherence between two diodes decreases as their separation increases. In Fig.4c, the coherence between diode #16 and the other diodes is plotted for three different frequency ranges. It can be seen that at 100 kHz the poloidal correlation length (defined as twice the poloidal separation at which the coherence falls to 0.6) is only about 2 cm, while at 50 kHz it is about 5 cm and at 20 kHz it is about 7 cm. This tendency for higher-frequency components to have smaller poloidal correlation lengths than the lower-frequency components is very similar to that observed for density fluctuations in the edge of Macrotor [6].

4. CORRELATION WITH THE LANGMUIR PROBE

The movable Langmuir probe was inserted into the plasma edge to a point near focus of photodiode #15 (see Fig.1), and its ion saturation current I_s was

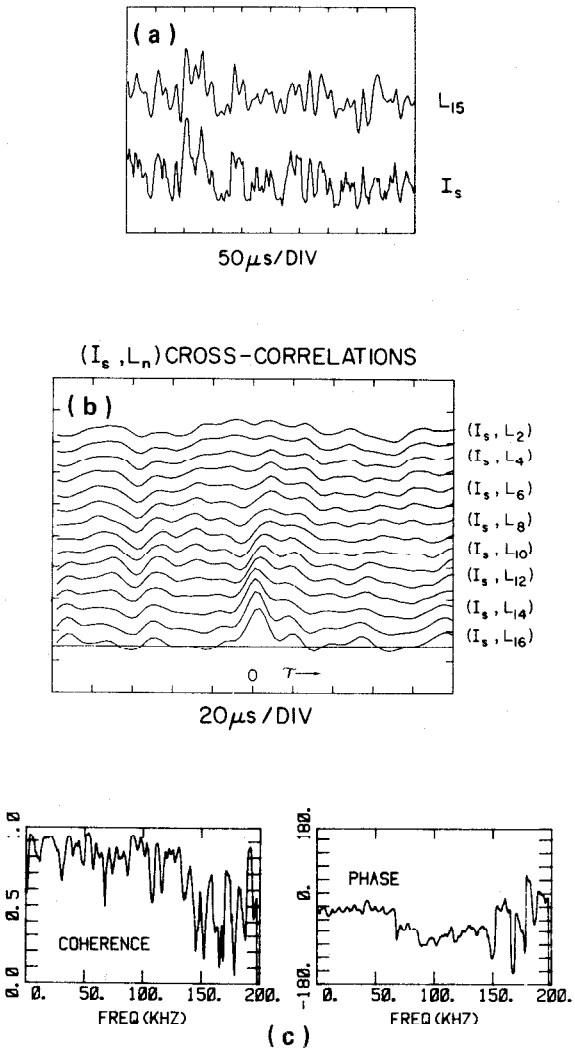

FIG.5(a). Signals from Langmuir probe and from photodiode #15 taken during middle portion of discharge; (b) cross-correlation functions between Langmuir probe and photodiodes; (c) coherence and phase spectra between Langmuir probe and photodiode #15.

recorded on one of the digitizer channels. Figure 5a shows an example of the comparison between the I_s signal and the photodiode signal L_{15} at $t \cong 6$ ms, showing that they are evidently quite well correlated (note that the bandwidth of the I_s signal is 200 kHz compared to 150 kHz for the photodiode signal). Although the data described here were taken with the probe tip inserted 0.5 cm into a limiterless discharge (as shown for Fig.2), similar results were obtained for other radial positions in the edge and for cases in which the probe was in the shadow of a limiter.

In Fig.5b, typical cross-correlation functions (I_s, L_n) calculated similarly to those in Fig.4a are shown. For photodiodes focused near to the probe tip, a band-averaged normalized correlation cross-coefficient of up to 0.8 at $\tau = 0$ was obtained. For photodiodes focused away from the tip, the correlation falls off with poloidal separation similarly to the (L_{16}, L_n) correlations of Fig.4a.

Some results from a frequency-resolved analysis between I_s and the nearest-focused photodiode signal (#15) have also been obtained. The spectral shapes of the two signals are similar below 80 kHz, although between 80 and 150 kHz the signal from L_{15} decreased somewhat more than that of I_s. As is shown in Fig.5c, the correlation between probe and L_{15} is high up to 150 kHz, and the phase between the two signals is nearly 0° up to at least 60 kHz. In general, the analysis of the correlation between the Langmuir probe and the photodiodes indicates that the probe fluctuations are very similar to those of the photodiode focused at its tip, at least below about 100 kHz.

5. CONCLUSIONS

The simplest interpretation of these results is that the visible light from this tokamak is fluctuating in response to density turbulence in the edge plasma. In particular, the high correlation and 0° phase between the probe and the photodiodes focused near to it shows a posteriori that the visible fluctuations are correlated with a local edge property of the plasma. The space-time patterns of edge plasma turbulence as observed using the visible light emission (see Figs 3 and 4) are also quite similar to those previously measured with probes in the edge plasma [6]. It might be argued that both signals could also be responding to temperature fluctuations; however, since the visible-light emission is a non-linear function of the plasma temperature, it is unlikely that the phase between the two would be so clearly 0° if temperature fluctuations were dominant.

Such imaging of plasma light emission patterns works well for small-scale structures in the plasma periphery since the optical system can provide good spatial resolution at the outer edge while averaging over small-scale structure away from the outer edge. In fact, the array also responds to large-scale coherent modes which occur before plasma disruption; however, the restricted access and the possibility of contributions from off the focal plane limit the usefulness of this system for studying large-scale modes.

Of course, the system described here also has the defect of integrating over any radial structure which might exist within the outer edge. It is possible that a two-dimensional array could be constructed to view tangentially to the field line both the poloidal and radial structure of the edge; however, the requirements of 2-D digital data acquisition quickly become formidable. Even with the 1-D system it is, however, possible to search for the existence of coherent structures within the apparent turbulence, such as have recently been discovered in fluid turbulence experiments [9].

Finally, the observation of turbulence through the use of the visible light emission has also allowed a non-perturbative check of the Langmuir probe results, which has shown that the local fluctuation pattern remains unchanged by the insertion of the probe into the edge plasma. For larger tokamaks even a single photodiode channel can provide a convenient monitor of edge plasma turbulence without the use of probes.

ACKNOWLEDGEMENT

We thank P.C. Liewer for many discussions about edge turbulence.

REFERENCES

[1] GOODALL, D.H.J., J. Nucl. Mater. **111/112** (1982) 11.

[2] NIEDERMEYER, H., ASDEX GROUP (1982), private communication (we thank H. Niedermeyer for providing us with a copy of one of his ASDEX films).

[3] SLUSHER, R.E., SURKO, C.M., Phys. Fluids **23** (1980) 2425.

[4] MAZZUCATO, E., Phys. Rev. Lett. **48** (1982) 1828.

[5] ZWEBEN, S., LIEWER, P.C., GOULD, R.W., J. Nucl. Mater. **111/112** (1982) 39.

[6] ZWEBEN, S.J., TAYLOR, R.J., Nucl. Fusion **21** (1981) 193.

[7] ZWEBEN, S.J., TAYLOR, R.J., Plasma Phys. **23** (1981) 337.

[8] BENDAT, J.S., PIERSOL, A.G., Random Data, Wiley-Interscience, 332.

[9] JIMENEZ, J. (Ed.), Role of Coherent Structures in Modelling Trubulence and Mixing, Lecture Notes in Physics No. 136 (1981), Springer-Verlag.

(Manuscript received 10 February 1983
Final manuscript received 26 April 1983)